Iron-Activated Alcohol Dehydrogenase from *Zymomonas mobilis*: Spectroscopic and Magnetic Properties

Eddy N. Bakshi,[1a,c] Peter Tse,[1b] Keith S. Murray,*[,1a] Graeme R. Hanson,[1a,d] Robert K. Scopes,[1b] and Anthony G. Wedd*[,1b]

Contribution from the Departments of Chemistry and Biochemistry, La Trobe University, Bundoora, Victoria, 3083, Australia, and Departments of Chemistry and Physics, Monash University, Clayton, Victoria, 3168, Australia. *Received February 13, 1989*

Abstract: The spectroscopic and magnetic properties of the active Fe^{II} and Co^{II} forms of the title enzyme are presented as well as those of the inactive Mn^{II}, Ni^{II}, and Cu^{II} forms. Magnetic susceptibility, ESR, Mössbauer, and electronic spectral data all point to the presence of high-spin six-coordinate sites influenced by a ligand field close to octahedral. The electronic spectra of M^{II}-ADH (M = Co, Ni) are closely related to those exhibited by the *cis*-MN_4O_2 sites in crystalline $M(His)_2 \cdot H_2O$. At least three and most probably four nitrogen ligands are observed directly via hyperfine structure in the ESR spectrum of Cu^{II}-ADH. Taken as a whole, the results strongly support the presence of a high-spin, six-coordinate ferrous site in the native enzyme. The three or four nitrogen ligands present would appear to be histidine residues, while the other ligands are most likely to be supplied by H_2O, aspartate, glutamate, or tyrosinate.

The previous paper in the issue[2] reported purification of the metal-free apo form of the title enzyme, designated ZADH-2, and definition of apparent dissociation constants for binding of bivalent first-row transition-metal ions to the apoenzyme: pK_M, 7.4-9.0; M = Mn^{2+}-Zn^{2+}. The tight binding and the low levels of adventitious metal contamination in the purified apoenzyme implies that a well-defined metalated derivative of ZADH-2, M^{II}-ADH, can be generated by addition of a single equivalent of metal ion per subunit of apoenzyme.

This paper reports spectroscopic and magnetic characterization of the species M^{II}-ADH. The work has been aided by the availability of apoenzyme to act as reference and diamagnetic correction, by the opportunity to introduce specific isotopes (^{57}Fe, ^{63}Cu), and by the fact that the samples can be generated just prior to examination.

Fe^{II}-ADH is of special interest as it is the native enzyme. It is shown to contain a six-coordinate high-spin ferrous site featuring a mixture of nitrogen (at least three and probably four) and oxygen ligand atoms, a striking contrast to the four-coordinate ZnS_2NO catalytic site of horse liver ADH (HLADH). Preliminary results have been communicated previously.[3]

Experimental Section

The apoenzyme was generated according to ref 2. The metalated enzymes, M^{II}-ADH, were generated from apoenzyme in metal-free[2] K-Mes buffer (10-50 mM; pH 6.5) by the addition of 1 equiv of spectroscopically pure metal salts, just prior to the physical measurements.

Electronic Spectroscopy. Spectra of M^{II}-ADH (M = Co, Ni, Cu) in the range 12 000-25 000 nm^{-1} were measured on a Cary 118C spectrophotometer equipped with quartz cuvettes of 4-cm path length.

Equal volumes of apo-ADH, of known protein concentration (1.98×10^{-4}-3.74×10^{-4} M), were pipeted into the reference and sample cells. The base line was then defined. One equivalent of metal ion in buffer was introduced to the sample cuvette. An equal volume of buffer was added to the reference.

Electron Spin Resonance. X-band spectra at 77 and 4.2 K were recorded for M^{II}-ADH (M = Mn, Co, Cu) on Varian E-9 and E-12 spectrometers. The magnetic field was calibrated against the proton magnetic resonance of H_2O, which was measured together with the microwave frequency on an EIP 548A frequency counter.

The signal to noise ratios for the EPR spectra of Co(II)-ADH and its complexes with NAD^+ and NAD^+/*i*-PrOH are quite low as a result of their inherently large line widths (see below). Increased signal to noise ratios were obtained through signal averaging on an LSI 11/23 computer linked to the VAX network at Monash University Computer Centre.

The spin Hamiltonian parameters and line-width parameters σ_R, C_{1i}, and C_{2i} were determined by computer simulation of the experimental EPR spectrum as outlined previously for high-spin Co(II) and Cu(II) complexes.[4,5] The actual line width in frequency units is

$$\sigma_i^2 = \sigma_{Ri}^2 + (C_{1i}\,\nu_0(B) + C_{2i}M_I)^2 \quad (1)$$

where $i = \perp$, $\parallel$, or, in general, x, y, z. The σ_R terms are residual line widths arising from dipolar broadening, unresolved metal and ligand hyperfine structure, or both, while C_{1i} and C_{2i} represent strain-induced distributions of g and A values.[6] $\nu_0(B)$ represents the field-dependent frequency difference between two energy levels. The line-width parameters used are listed here in order to properly define the simulations (σ_{Ri} and C_{2i} are in MHz while C_{1i} are dimensionless):

	$\sigma_{R\parallel}$	$\sigma_{R\perp}$	$C_{1\parallel}$	$C_{1\perp}$	$C_{2\parallel}$	$C_{2\perp}$
Co^{II}-ADH	166.4	247.5, 128.1	0.120	0.191, 0.269	0	0, 0
Co^{II}-ADH-NAD^+	161.4	513.3	0	0.185	0	0
Cu^{II}-ADH	49.70	10.19	0.011	-0.003	46.35	28.01

An estimation of the quality of fit of a simulation (S) to an experimental spectrum (E) was provided by the least-squares error parameter (L), defined in eq 2:

$$L = [(E/I_E) - (S/I_S)]^2/N \quad (2)$$

where I_E and I_S are the normalization factors (doubly integrated intensities) and N is the number of points in both the simulated and experimental spectra.

An aqueous solution of $^{63}Cu(NO_3)_2$ was prepared by dissolving CuO (70 mg; 99.89 atom % ^{63}Cu) purchased from Oak Ridge National Laboratories, Oak Ridge, TN, in concentrated HNO_3 (0.2 cm^3). The solution was made up to 100 cm^3 with metal-free K-Mes buffer.

Magnetic Susceptibility. Measurements were effected on a SCT SQUID susceptometer[7] operating at 115.2 mT applied field. Calibration of field and temperature employed freshly crystallized solid samples of $CuSO_4 \cdot 5H_2O$ ($\chi = 0.4580/(T - 0.7)$)[8] and $MnCl_2 \cdot 4H_2O$ ($\chi = 4.3770/(T + 2)$).[9] A single quartz sample tube (0.3 $cm^2 \times 6$ cm) was used for all measurements on 0.3-cm^3 samples derived from the same stock of apo-ADH (subunit concentration, 1.01×10^{-3} M). Calibration of effective sample volume between the pickup coils was made with $Mn(CH_3CO_2)_2 \cdot 4H_2O$[10] dissolved in the enzyme buffer. Solutions of $Cu(NO_3)_2$[11]

(1) (a) Monash University. (b) La Trobe University. (c) Present address: Dept. of Physics, Swinburne Institute of Technology, Hawthorn, Victoria, 3122, Australia. (d) Present address: Dept. of Inorganic Chemistry, University of Queensland, St. Lucia, Queensland, 4067, Australia.

(2) Tse, P.; Scopes, R. K.; Wedd, A. G. *J. Am. Chem. Soc.*, preceding article in this issue.

(3) Tse, P.; Scopes, R. K.; Wedd, A. G.; Bakshi, E.; Murray, K. S. *J. Am. Chem. Soc.* **1988**, *110*, 1295-1297.

(4) Martinelli, R. A.; Hanson, G. R.; Thompson, J. S.; Holmquist, B.; Pilbrow, J. R.; Auld, D. S.; Vallee, B. L. *Biochemistry* **1989**, *28*, 2251-2258.

(5) Dougherty, G.; Pilbrow, J. R.; Skorobogarty, A., Smith, J. D. *J. Chem. Soc., Faraday Trans. 2* **1985**, *81*, 1739-1759.

(6) Froncisz, W.; Hyde, J. S. *J. Chem. Phys.* **1980**, *73*, 3123-3131.

(7) Gregson, A. K.; Doddrell, D. M.; Healey, P. C. *Inorg. Chem.* **1978**, *17*, 1216-1219.

(8) Arts, H. J. J. M.; van der Steen, C.; Poulis, J. A.; Massen, C. H. *Appl. Sci. Res.* **1974**, *29*, 290.

(9) Gijsman, H. M.; Poulis, N. J.; van der Handel, J. *Physica* **1954**, *25*, 954.

0002-7863/89/1511-8707$01.50/0

Table I. Mössbauer Parameters for Fe^{II} Centers (mm s^{-1}) at 4.2 K

system	δ (±0.004)	ΔE_Q (±0.01)	Γ_l[a]	Γ_h[a]	I_l/I_h[b]	ref
Fe^{II}-ADH	1.24	3.43	0.26	0.20	1.13	*i*
Fe^{II}-ADH:NAD^+ (1:3.4)	1.25	3.33	0.24	0.23	1.08	*i*
Fe^{II}-ADH:NAD^+:*i*-PrOH (1:3.4:2600)	1.24	3.30	0.20	0.17	1.18	*i*
Fe^{II}-HLADH (species I)	0.86	3.82				23, 24
Fe^{II}-HLADH (species II)[h]	1.31	3.35				
rubredoxin[c]	0.70	3.25				25
catechol 2,3-dioxygenase[d]	1.31	3.28				26
protocatechuate 3,4-dioxygenase[e]	1.21	3.13				27
protocatechuate 4,5-dioxygenase[f]	1.28	2.22				22
photosynthetic reaction center[g]	1.17	2.22				28

[a] Half-widths of the lower (l) and higher (h) velocity components. Minimum experimental line widths were 0.20 mm s^{-1} for Fe^{II}-ADH and 0.12 mm s^{-1} for the other species. [b] Ratio of integrated intensities. [c] *Clostridium pasteurianum.* [d] *Pseudomonas arvilla.* [e] *P. aerugenosa.* [f] *P. testerostoni.* [g] *Rhodopseudomonas sphaeroides* R_{26}. [h] This species is incompletely characterized at present.[23] [i] This work.

in buffer and $MnCl_2 \cdot 4H_2O$ in 0.2 M hydrochloric acid[9] confirmed the effective volume. The high-temperature limit of measurement was determined by the detectable magnetization of each individual sample but was always less than 60 K for these simple paramagnets at the available subunit concentration.

The diamagnetic correction at each temperature was determined by measurement of magnetization of a combination of apo-ADH, buffer, and the quartz sample tube. The samples themselves differed by the addition of 1 equiv of metal salt. All but one of the potential sources of noise in such SQUID measurements[12] have been eliminated in the present case. The use of deuterated buffer and solvent is desirable to reduce the effects of the long relaxation time of protons in aqueous buffer, but was not employed here. However, such effects were negligible in a recent study of Ni^{II} enzymes having similar magnetic and structural properties to Ni^{II}-ADH.[13]

Mössbauer Spectroscopy. A constant acceleration spectrometer[14] was employed. Background contributions to the spectra were zero. Calibration was made with respect to α-iron. Applied fields were oriented parallel to the direction of the γ-iron radiation with the source position in zero field. Samples (1-cm^3 volume) were placed in Teflon containers, which could be kept frozen and evacuated during insertion into the cryostat sample chamber. Line shapes were fitted by a least-squares program utilizing Lorentzian functions.

Samples of $^{57}Fe^{II}$-ADH and $^{57}Fe^{III}$-ADH [(0.62–1.01) × 10^{-3} M; 95.44 atom % ^{57}Fe] were generated by addition of 1 equiv of solution of $(NH_4)_2Fe(SO_4)_2$ or $Fe(NO_3)_3$ to apo-ADH. The latter salts were prepared from metal produced by hydrogen reduction of $^{57}Fe_2O_3$ (Oak Ridge National Laboratories).

The ferrous salt was prepared by anaerobic oxidation of the metal (22 mg) with H_2SO_4 (1 M; 4 cm^3) for 8 h. $FeSO_4$ was isolated by precipitation with oxygen-free EtOH (10 cm^3) at 4 °C followed by removal of supernatant, washing three times with EtOH and drying under vacuum. Metal-free K-Mes buffer (3 cm^3; 10 mM; pH 6.5) containing $(NH_4)_2SO_4$ (51 mg) was added to form the ferrous solution, which was stored anaerobically at 4 °C. The total Fe concentration of the solution was determined by atomic absorption spectroscopy and the Fe^{II} and Fe^{III} concentrations by colorimetry:[15] total Fe, 0.106 M; Fe^{II}, 0.099 M; Fe^{III} <0.002 M.

The ferric salt was prepared by dissolving the metal (7.2 mg) in hot HNO_3 (6 M; 1 cm^3). After evaporation to near dryness, the volume was taken to 5 cm^3 with distilled water. Total Fe, 0.020 M; Fe^{II}, <0.001 M; Fe^{III}, 0.020 M.

Results and Discussion

Apo-ADH. Prior to each physical measurement, the activity of an aliquot of the apoenzyme reconstituted[2] with Fe^{II} or Co^{II} was measured to confirm that the particular sample could be fully reactivated. ESR signals could not be detected in the apoenzyme at 77 or 4.2 K, nor could a Mössbauer signal be detected in the apoenzyme at 4.2 K. The magnetization of apo-ADH in the range 4.2–60 K at a field strength of 116.05 mT was that characteristic of a diamagnetic substance.

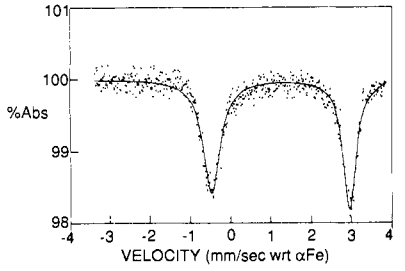

Figure 1. Mössbauer spectra of Fe^{II}-ADH (1.01 mM; 95.4 atom % ^{57}Fe) at 4.2 K and no applied field.

The Native Enzyme, Fe^{II}-ADH. No electronic absorption was detected in the range 12 000–25 000 cm^{-1}, eliminating the possibility of five-coordinate or low-spin six-coordinate iron(II) sites.[16a,b]

The Mössbauer spectrum (Table I; Figure 1) at 4.2 K and zero field shows a single, quadrupole doublet whose asymmetry is most likely due to a distribution of microscopic isomer shifts and quadrupole splittings in the frozen sample. The observed isomer shift δ, 1.243 (4) mm s^{-1}, and quadrupole splitting ΔE_Q, 3.43 (1) mm s^{-1}, are typical[17–20] of high-spin $S = 2$ ferrous centers in a ligand field close to octahedral. They are also close to those reported for "free" Fe^{2+} in reducing buffer solutions:[21,22] this possibility is unlikely in view of the high activity of the ligand sample before and after measurement.

Comparison of the Mössbauer parameters with those observed for other mononuclear, high-spin ferrous centers (Table I) suggests that the sites in Fe^{II}-ADH, catechol 2,3-dioxygenase,[26] and protocatechuate 3,4-dioxygenase[27] are related. The parameters for this group differ significantly from those of (i) Fe^{II}-HLADH

(10) Flippen, R. B.; Friedberg, S. A. *Phys. Rev.* **1961**, *121*, 1591–1598.
(11) König, E. *Landolt Börnstein Tables*; Springer Verlag: New York, 1984; Vol. 11, Group 11, pp 2–323.
(12) Day, E. P.; Kent, T. A.; Lindahl, P. A.; Münck, E.; Orme-Johnson, W. H.; Roder, H.; Roy, A. *Biophys. J.* **1987**, *52*, 837–853.
(13) Clark, P. A.; Wilcox, D. E. *Inorg. Chem.* **1989**, *28*, 1326–1333.
(14) Mitchell, A. J.; Murray, K. S.; Newman, P. J.; Clarke, P. E. *Aust. J. Chem.* **1977**, *30*, 2439–2453.
(15) Vogel, A. I. *A Textbook of Quantitative Inorganic Analysis*, 4th ed.; Longman: London, **1978**; pp 741–743.
(16) Lever, A. B. P. *Inorganic Electronic Spectroscopy*, 2nd ed.; Elsevier: Amsterdam, 1984; pp (a) 462–470, (b) 470–471, (c) 480–505, (d) 507–544, (e) 680–687.
(17) Long, G. J. In *Mössbauer Spectra Applied to Inorganic Chemistry*; Long, G. J., Ed.; Plenum: New York, 1984; pp 7–26.
(18) Dickson, D. P. E. ref 17, pp 339–389.
(19) Huynh, B. H.; Kent, T. A. *Adv. Inorg. Biochem.* **1985**, *6*, 163–223.
(20) Menil, F. *J. Phys. Chem. Solids* **1985**, *46*, 763–789.
(21) Kent, T. A.; Dreyer, J. L.; Kennedy, M. C.; Huynh, B. H.; Emptage, M. H.; Beinert, H.; Münck, E. *Proc. Natl. Acad. Sci. U.S.A.* **1982**, *79*, 1096–1100.
(22) Arciero, D. M.; Lipscomb, J. D.; Huynh, B. H.; Kent, T. A.; Münck, E. *J. Biol. Chem.* **1983**, *258*, 14981–14991.
(23) (a) Haas, C.; Dietrich, H.; Maret, W.; Zeppezauer, M.; Montiel-Montoya, R.; Bill, E.; Trautwein, A. X. *Hyperfine Interact.* **1986**, *29*, 1419–1422. (b) Bill, E.; Ding, X.-Q.; Haas, C.; Winkler, H.; Trautwein, A. X.; Zeppezauer, M. *Hyperfine Interact.* **1988**, *42*, 877–880.
(24) Bill, E.; Claus, H.; Ding, X.-Q.; Maret, W.; Winkler, H.; Trautwein, A. X.; Zeppezauer, M. *Eur. J. Biochem.* **1989**, *180*, 111–121.
(25) Debrunner, P. G.; Münck, E.; Que, L., Jr.; Schulz, C. E. In *Iron–Sulfur Proteins*; Lovenberg, W., Ed.; Academic Press: London, New York, 1976; Vol. 3, pp 381–417.
(26) Tatsuno, Y.; Saeki, Y.; Nozaki, M.; Otsuka, S.; Maeda, Y. *FEBS Lett.* **1980**, *112*, 83–85.
(27) Que, L., Jr.; Lipscomb, J. D.; Ziemmerman, R.; Münck, E.; Orme-Johnson, M. R.; Orme-Johnson, W. H. *Biochim. Biophys. Acta* **1976**, *452*, 320–334.

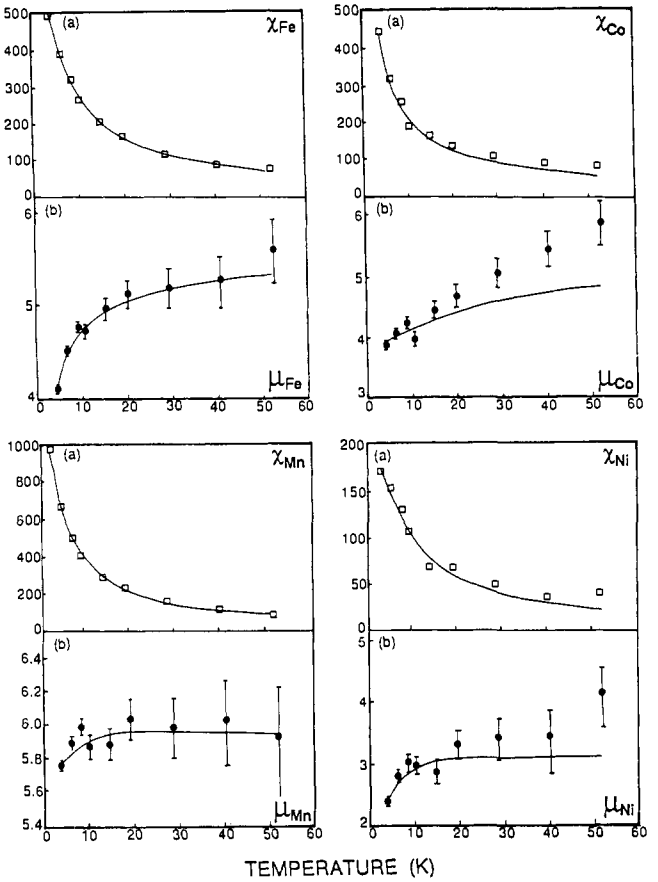

Figure 2. Temperature dependence of (a) magnetic susceptibility, 10^{-3} cm^3 (g atom)$^{-1}$ and (b) magnetic moment, μ_B, in Fe^{II}-, Co^{II}-, Mn^{II}-, and Ni^{II}-ADH in the range 4.2–52 K. Solid lines are the plots of best fit calculated from parameters given in the text, and in the Appendix.

(species I)[23,24] and rubredoxin[25] and (ii) protocatechuate 4,5-dioxygenase[22] and a bacterial photosynthetic reaction center.[28] Both Fe^{II}-HLADH and rubredoxin feature a coordination number less than six and a number of cysteinyl ligands. On the other hand, the six-coordinate [$Fe(His)_4(Glu)$] site in the photosynthetic reaction center[29,30] might be expected to display a value of ΔE_Q similar in magnitude to that of Fe^{II}-ADH, and the observed difference may reflect the small bite angle of the bidentate glutamate ligand.

The temperature dependence of the magnetic moment and susceptibility of Fe^{II}-ADH in the range 4–52 K is shown in Figure 2. Curie–Weiss behavior is observed (θ, −3.5 K) with $\mu_{Fe} \sim 5.2$ μ_B in the range 20–50 K falling to 4.1 μ_B at 4.2 K. The data confirm the high-spin ferrous state. The overall behavior is consistent with an octahedral $^5T_{2g}(d^6)$ ground state whose orbital degeneracy has been raised by a combination of spin–orbit coupling (λ) and a lower symmetry ligand field (Δ and R, axial and rhombic parameters, respectively).[31] The data could be fitted well to such a model[31] (see Appendix). The final set of best-fit values of the parameters, represented by the solid lines in Figure 2, is

$$\lambda = -120\ cm^{-1} \quad \Delta = 740\ cm^{-1} \quad R = 330\ cm^{-1} \quad \kappa = 1$$
$$I = 2.1\%$$

κ is the orbital reduction factor, and I is a discrepancy index (see Appendix). The parameters indicate that the parent $^5T_{2g}$ state is split by an axial ligand field component to yield an orbital singlet lowest while the upper doublet is further split by a large rhombic component. A rhombic component was also needed[24] to get a good fit in a spin Hamiltonian analysis of the applied field Mössbauer spectrum of Fe^{II}-HLADH. However, the magnitude of the rhombic component was smaller, relative to the axial component, than is the case here. Furthermore, it appears that the axial parameter in Fe^{II}-ADH is much bigger and possibly of opposite sign to that for the HLADH case, although susceptibility measurements are not available to confirm this. The results again suggest significant differences between the two systems.

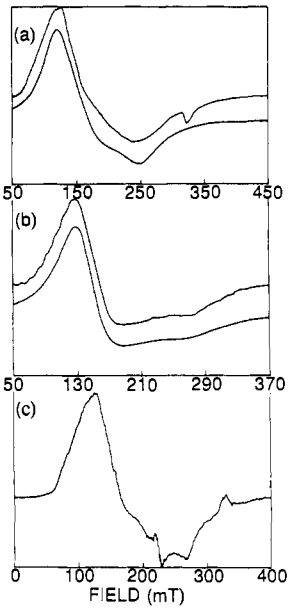

Figure 3. ESR spectra of Co^{II}-ADH systems. (a) Co^{II}-ADH; (b) Co^{II}-ADH:NAD^+ (1:3.4); (c) Co^{II}-ADH:NAD^+:*i*-PrOH (1:3.4:2600). Temperature, 9.5 K; microwave frequency, 9.159 GHz; Co concentration, 5.9×10^{-4} M. (a) and (b) include simulations of the experimental spectra. Derived g values are in Table II.

Interestingly, susceptibility measurements on native soybean lipoxygenase-1 (SBL) between 10 and 170 K gave a set of best-fit spin Hamiltonian parameters rather similar to those for Fe^{II}-HLADH, indicative of an essentially axially symmetric ligand environment for the high-spin Fe^{II} site.[33] However, recent MCD studies on SBL by Whittaker and Solomon[34] (over the range 1.6–12 K, H = 0–6 T) show that a ligand field analysis of the type used here for Fe^{II}-ADH is required, rather than a spin Hamiltonian approach, since the symmetry around Fe^{II} is close to octahedral. The axial and rhombic splittings for SBL derived from the MCD work[34] were found to be of a magnitude similar to those seen here for Fe^{II}-ADH, but significantly, the axial splitting was of opposite sign i.e., orbital doublet lowest. The results suggest subtle geometric differences between the Fe^{II} sites in ZADH-2 and SBL.

Co^{II}-ADH. This form of the enzyme is catalytically competent,[2] being ~45% as active as the native ferrous enzyme.

The magnetic moment of Co^{II}-ADH is very temperature dependent, decreasing from $\sim 5.5 \pm 0.5$ μ_B at 40–50 K to 3.9 ± 0.1 μ_B at 4.2 K (Figure 2). The behavior is that expected for a high-spin $^4T_{1g}(d^7)$ octahedral ground state split by spin–orbit coupling and a low symmetry ligand field component. The data were analyzed by using the same model employed for Fe^{II}-ADH (see Appendix). Exploration of wide variations in the parameters showed that, for best fit (I − 7%)

$$\lambda \sim -50\ cm^{-1} \quad |\Delta| \sim 70\ cm^{-1} \quad R \sim 0\text{–}40\ cm^{-1}$$
$$\kappa \sim 1$$

(28) Boso, B.; Debrunner, P.; Okamura, M. Y.; Feher, G. *Biochim. Biophys. Acta* **1981**, *638*, 173–177.
(29) Deisenhofer, J.; Epp, O.; Miki, K.; Huber, R.; Michel, H. *Nature* **1985**, *318*, 618–624.
(30) Allen, J. P.; Feher, G.; Yeates, T. O.; Komiya, H.; Rees, D. C. *Proc. Natl. Acad. Sci U.S.A.* **1987**, *84*, 5730–5734.
(31) Mabbs, F. E.; Machin, D. J. *Magnetism and Transition Metal Complexes*; Chapman and Hall: London, 1973; Chapter 5.
(32) Bohan, T. L. *J. Magn. Reson.* **1977**, *26*, 109–118.
(33) Petersson, L.; Slappendel, S.; Vliegenthart, J. F. G. *Biochim. Biophys. Acta* **1985**, *828*, 81–85.
(34) Whittaker, J. W.; Solomon, E. I. *J. Am. Chem. Soc.* **1988**, *110*, 5329–5339. Notation: Δ and V in this paper is equivalent to our $\Delta/3$ and $R/6$.

Table II. ESR g Values for Co^{II}-ADH and Related Enzyme Systems

system	g_1	g_2	g_3	ref
Co^{II}-ADH[a]	5.22	3.78	2.55	c
Co^{II}-ADH:NAD^+ (1:3.4)[a]	4.53	4.53	2.40	c
Co^{II}-ADH:NAD^+:*i*-PrOH (1:3,4:2600)[b]	5.2	3.6	2.9	c
glyoxylase I	6.6	3.0	2.5	40
alkaline phosphatase	6.36	3.4	2.66	41
phospholipase *C*	6.87	2.72	1.99	38
enolase	3.97	2.67	2.06	39

[a] Determined by computer simulation of the experimental spectrum. [b] Measured directly from the spectrum. [c] This work.

Table III. Electronic Spectra of Co^{II}-ADH Systems

system	λ_{max}, cm^{-1}	ϵ, M^{-1} cm^{-1}
Co^{II}-ADH	16 300 (sh)	3.6
	19 000	30.4
	19 600	31.5
	21 300	23.2
Co^{II}-ADH:NAD^+ (1:3.4)	16 700 (sh)	50
	17 500	71
	18 900 (sh)	44
Co^{II}-ADH:NAD^+:*i*-PrOH (1:3.4:2600)	17 500 (sh)	125
	18 000	143
	19 600	89
	20 700 (sh)	75
Co^{II}-glyoxylase I[a]	16 300	8
	19 400	33
	20 300	35
	21 500	26

[a] Reference 40.

While the parameters are subject to large uncertainties (see Appendix), nevertheless, the analysis clearly indicates the presence of a ligand field close to octahedral with weakly covalent cobalt ligand bonding ($\kappa \sim 1$).

The ESR spectrum of Co^{II}-ADH is shown in Figure 3a. Satisfactory simulation with an effective $S = {}^1/_2$ spin Hamiltonian indicates that the transitions arise from within a single Kramers doublet. The derived g values are listed in Table II and the line-width parameters are given in the Experimental Section.

The line widths of these resonances are fairly sensitive to temperature and the ESR spectrum is virtually undetectable above 40 K. This temperature dependence, the large line widths, and the highly anisotropic g values are those expected for a high-spin ground state and distorted octahedral geometry. The conclusions are supported by comparison with model systems[35-37] and with Co^{II}-substituted enzymes proposed to have six-coordinate sites featuring nitrogen and oxygen ligands (Table II).[38-41]

The electronic spectrum of Co^{II}-ADH, relative to apo-ADH as reference, is presented in Figure 4 and Table III. The presence of an absorption maximum at $\sim$20 000 cm^{-1} with $\epsilon < 50$ M^{-1} cm^{-1} is strong evidence for a high-spin, six-coordinate site.[16c,35,42] This maximum is normally assigned to the $^4T_{1g}(F) \rightarrow {}^4T_{1g}(P)$ transition of octahedral symmetry. However, in many cases,[16c,35] the band envelope is multiply structured with contributions arising from a number of sources such as forbidden transitions and the raising of state degeneracies via spin–orbit coupling and lower symmetry ligand fields.

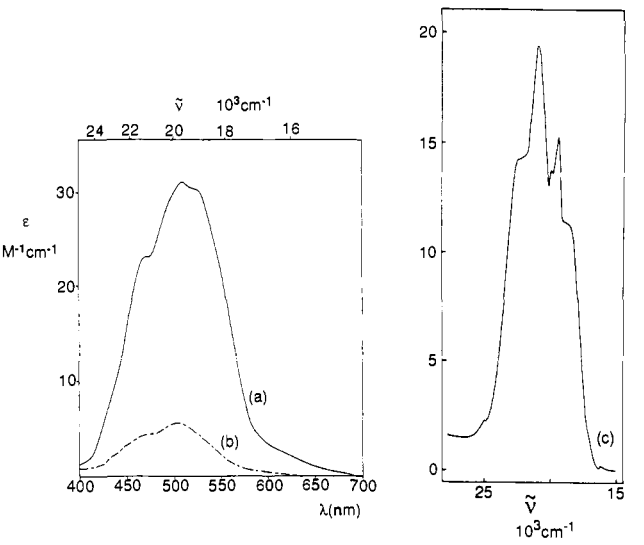

Figure 4. Electronic spectra. (a) Co^{II}-ADH; (b) $[Co(H_2O)_6]^{2+}$, aqueous solution; (c) Co(L-His)$_2$·H_2O, single crystal, 80 K (adapted from ref 43 with permission).

Table IV. Comparison of the Electronic Spectra of Co^{II}-ADH and Co(L-His)$_2$·H_2O

Co(L-His)$_2$·H_2O[a]	assignment[b]	Co^{II}-ADH
18 700	$^4T_{1g}(P)$	
19 300		18 800–19 000
19 600	$^2T_{2g}(G)$	
19 800		
20 800	$^4T_{1g}(P)$	19 600
22 300	$^4A_{2g}$	21 300

[a] Reference 43. [b] For simplicity, the parent octahedral excited states are listed.

The magnetic and ESR results discussed above suggest that the last effect at least is relevant to Co^{II}-ADH, and comparison with $[Co(H_2O)_6]^{2+}$ (Figure 4a,b) confirms the lower symmetry: the number of unresolved components in the band envelope has increased and the absorption is more intense due to relaxation of the Laporte selection rule.

The weak shoulder at 16 300 cm^{-1} in Co^{II}-ADH is plausibly assigned to the equivalent of the forbidden two-electron transition $^4T_{1g}(F) \rightarrow {}^4A_{2g}(F)$ seen in the same region in $[Co(H_2O)_6]^{2+}$ and other complexes.[16c] However, this transition may in fact be contributing to the more intense absorption at 21 300 cm^{-1} as the observed band envelope of Co^{II}-ADH is similar in shape to but less well resolved than that of crystalline Co(L-His)$_2$·H_2O (Figure 4c), which features a *cis*-N_4O_2 coordination sphere.[43] The polarized crystal spectrum of this complex has been analyzed by assuming C_{2v} symmetry and the six most intense features have been assigned to transitions arising from the parent $^4T_{1g}(F) \rightarrow {}^4T_{1g}(P)$, $^2T_{1g}(^2G)$ and $^4A_{2g}$ transitions of octahedral symmetry. Table IV summarizes the comparison of Co^{II}-ADH and Co(L-His)$_2$·H_2O and provides a plausible assignment of the Co^{II}-ADH spectrum.

When compared to other Co^{II}-substituted enzymes, the Co^{II}-ADH spectrum bears close resemblance to those of conalbumin,[42] phospholipase C,[38] enolase,[39] and glyoxylase I.[40] Comparison with the latter is particularly striking (Table III) and glyoxylase I is proposed to feature a N_2O_4 ligand set, including two rapidly exchanging water ligands.[40] In addition, the Co^{II}-ADH spectrum is very different from that of Co^{II}-HLADH (λ_{max}, 15 400 cm^{-1}; ϵ, 1200 M^{-1} cm^{-1}),[44] and the absence of intense charge-transfer bands at energies below 30 000 cm^{-1} indicates that cysteine is not a ligand. Preliminary magnetic circular dichroism mea-

(35) Banci, L.; Bencini, A.; Benelli, C.; Gatteschi, D.; Zanchini, C. *Struct. Bonding* **1982**, *52*, 37–86.
(36) Makinen, M. W.; Kuo, L. C.; Yim, M. B.; Wells, G. B.; Fukuyama, J. M.; Kim, J. E. *J. Am. Chem. Soc.* **1985**, *107*, 5245–5255.
(37) Kuo, L. C.; Makinen, M. W. *J. Am. Chem. Soc.* **1985**, *107*, 5255–5261.
(38) Bicknell, R.; Hanson, G. R.; Holmquist, B.; Little, C. *Biochemistry* **1986**, *25*, 4219–4223.
(39) Rose, S. L.; Dickinson, L. C.; Westhead, E. W. *J. Biol. Chem.* **1984**, *259*, 4405–4413.
(40) Sellin, S.; Eriksson, L. E. G.; Aronsson, A.-C.; Mannervik, B. *J. Biol. Chem.* **1983**, *258*, 2091–2093.
(41) Simpson, R. T.; Vallee, B. L. *Biochemistry* **1968**, *17*, 4343–4350.
(42) Bertini, I.; Luchinat, C. *Adv. Inorg. Biochem.* **1985**, *6*, 71–111.
(43) Meredith, P. L.; Palmer, R. A. *Inorg. Chem.* **1971**, *10*, 1546–1549.
(44) Maret, M.; Andersson, I.; Dietrich, H.; Schneider-Bernlöhr, H.; Einarsson, R.; Zeppezauer, M. *Eur. J. Biochem.* **1979**, *98*, 501–512.

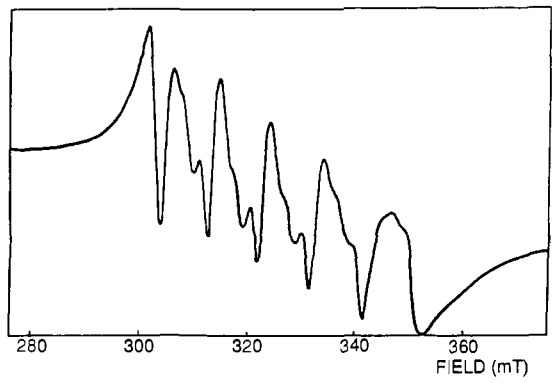

Figure 5. ESR spectrum of Mn^{II}-ADH at 77 K. Microwave frequency, 9.170 GHz.

surements confirm this finding.[45]

The physical data for the resting active enzymes, Fe^{II}-ADH and Co^{II}-ADH, point to the presence of mononuclear, high-spin, six-coordinate metal sites bound to oxygen and nitrogen ligands. While the other metalated forms of the enzyme are inactive, their physical properties were examined to provide extra insights into the nature of the active site.

Mn^{II}-ADH. The magnetic behavior is precisely that expected for a $^6A_{1g}(d^5)$ ground state. The susceptibility follows a strict Curie law ($\theta = 0$ K) and the moment is $5.9 \pm 0.2\ \mu_B$ in the range 50–15 K. Despite the large errors at the high-temperature end of the range, a small decrease due to zero field splitting is apparent below 15 K, reaching $5.74\ \mu_B$ at 4.2 K (Figure 2). The data were fitted to a spin Hamiltonian model (see Appendix) and the best fit parameters (Figure 2) were

$$g = 2 \qquad |D| = 1.4\ cm^{-1} \qquad I = 1.53\%$$

The value of the zero field splitting parameters $|D|$ suggests a slight deviation from octahedral symmetry at the Mn^{II} site. A more precise estimate of $|D|$ requires field-dependent magnetization studies[12,46,47] and an improvement in the signal to noise level.

The ESR spectrum (Figure 5) at 77 K shows the six-line ($I = {}^5/_2$) hyperfine structure at $g \sim 2$ characteristic of Mn^{II} centers[48,49] together with weaker features corresponding to forbidden transitions ($\Delta M_s > \pm 1$). The assumption of an isotropoic g tensor allows estimation of the g value (2.045) and the hyperfine coupling constant ($90 \times 10^{-4}\ cm^{-1}$). The additional assumption of an axial distortion from *Oh* symmetry provides an upper limit to the zero field splitting parameter, $|D| < 200 \times 10^{-4}\ cm^{-1}$. This estimate is more precise than that obtained from the susceptibility data since the resonances at ~115 and 700 mT predicted[47] if $|D| \sim 1\ cm^{-1}$ were not observed. In any case, deviation from cubic symmetry is slight. The spectrum is similar to that of certain forms of Mn^{II}-substituted phosphoglucomutase,[50] an enzyme thought to feature a N_2O_4 coordination sphere.

Ni^{II}-ADH. The magnetic moments of Ni^{II}-ADH cover a range of 2.4–~3.6 μ_B in the temperature interval 4–53 K as expected for a high-spin, six-coordinate Ni^{II} center. The susceptibilities follow the Curie–Weiss law with $\theta \sim -4.5$ K (Figure 2). Note the large errors at higher temperatures due to the weaker magnetization of the $S = 1$ system. The data could be fitted well to a spin Hamiltonian model (see Appendix) with the parameters

$$g = 2.2 \qquad |D| = 9\ cm^{-1} \qquad I = 9\%$$

The electronic spectrum of Ni^{II}-ADH relative to apo-ADH as reference is provided in Table V and Figure 6. In the 14 000–17 500-cm^{-1} range, the band envelope is similar in shape to that of $[Ni(H_2O)_6]^{2+}$. In the latter species, the two components are assigned to the $^3A_{2g} \rightarrow {}^3T_{1g}(F)$, ^1E_g transitions in which the two excited states are mixed by spin–orbit coupling.[16d] However, the higher intensity for Ni^{II}-ADH ($\epsilon = 12$ vs 2 $M^{-1}\ cm^{-1}$) indicates that a symmetry lower than cubic is relaxing the Laporte selection rule.

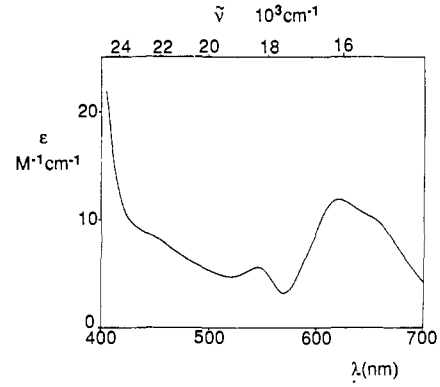

Figure 6. Electronic spectrum of Ni^{II}-ADH.

Table V. Electronic Spectra of Ni^{II}-ADH and Cu^{II}-ADH

system	λ_{max}, cm^{-1}	ϵ, $M^{-1}\ cm^{-1}$
Ni^{II}-ADH	15 300 (sh)	10.2
	16 100	12.0
	18 200	5.7
	22 300 (sh)	8.1
Cu^{II}-ADH	14 100	57

The Ni^{II}-ADH spectrum is also similar in band shape and intensity to that of crystalline $Ni(DL\text{-}His)_2 \cdot H_2O$, which features a *cis*-N_4O_2 coordination sphere.[51] The spectrum of the complex has been analyzed by assuming C_{2v} symmetry, and in contrast to the $[Ni(H_2O)_6]^{2+}$ ion, the states arising from the ^1E_g state of *Oh* symmetry are sufficiently removed from those arising from the $^3T_{1g}(F)$ state that mixing can be ignored.[51] The more intense absorptions in the 15 000–20 000- and 14 000–17 500-cm^{-1} ranges for the complex and enzyme systems, respectively, can then be assigned to transitions to the states derived from $^3T_{1g}(F)$. In addition, the weaker absorptions in the respective ranges 21 000–24 000 and 18 000–22 000 cm^{-1} are attributed to transitions to states derived from $^1A_{1g}(G)$ and $^1T_{2g}$.

Cu^{II}-ADH. The electronic spectrum (Table V) shows a broad band with a maximum absorption at 14 000 cm^{-1}, typical of simple Cu^{II} complexes. The molar absorptivity of 57 $M^{-1}\ cm^{-1}$ may indicate the presence of nitrogen ligands.[52,53] Certainly, the intense absorption ($\epsilon \sim 5000\ M^{-1}\ cm^{-1}$) seen in the 12 000–21 000-cm^{-1} region for type I copper proteins such as plastocyanin[16e] is absent. The latter contains a distorted tetrahedral CuN_2S_2 environment. Interestingly, the Cu^{II} form of HLADH is regarded as one of the best existing models of a type I copper site in proteins,[54] and its electronic spectrum features high-intensity absorptions at 16 100 (2000), 22 600 (500), and 26 500 (600) cm^{-1} ($M^{-1}\ cm^{-1}$). The contrast with the present Cu^{II}-ADH system is striking and provides further evidence for the absence of sulfur ligands.

$^{63}Cu^{II}$-ADH exhibits a very clean ESR spectrum (Figure 7) as a consequence of the presence of a single Cu isotope and of a single mononuclear copper species. The low field $M_I = {}^3/_2$ component of the parallel region of the spectrum will have the narrowest line width at X-band frequencies[6] and so is most likely to reveal the presence of fine structure due to ligand hyperfine

(45) Bicknell, R.; Holmquist, B.; Scopes, R. K., unpublished observations.
(46) Kennedy, B. J.; Murray, K. S. *Inorg. Chem.* **1985**, *24*, 1552–1557.
(47) Reedijk, J.; Klaaijsen, F. W.; Witteven, H. T. *J. Chem. Soc., Faraday Trans. 2* **1973**, *69*, 1537–1541.
(48) Palmer, G. *Biochem. Soc. Trans.* **1985**, *13*, 548–560.
(49) Reed, G. H.; Markham, G. D. *Biol. Magn. Reson.* **1984**, *6*, 77–87.
(50) Reed, G. H.; Ray, W. J. *Biochemistry* **1971**, *10*, 3190.
(51) Meredith, P. L.; Palmer, R. A. *Inorg. Chem.* **1971**, *10*, 1049–1056.
(52) Bernaducci, E.; Schwindinger, W. F.; Hughey, J. L.; Krogh-Jesperson, K.; Schugar, H. J. *J. Am. Chem. Soc.* **1981**, *103*, 1686–1691.
(53) Bernaducci, E.; Bharadwaj, P. K.; Krogh-Jesperson, K.; Potenza, J. A.; Schugar, H. J. *J. Am. Chem. Soc.* **1983**, *105*, 3860–3866.
(54) Maret, W.; Dietrich, H.; Ruf, H.-H.; Zeppezauer, M. *J. Inorg. Biochem.* **1980**, *12*, 241–252.

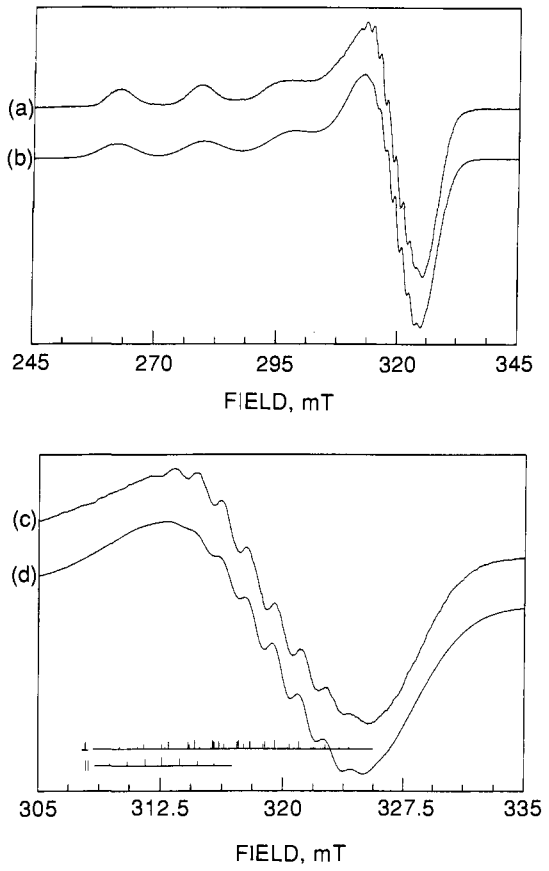

Figure 7. ESR spectrum of $^{63}Cu^{II}$-ADH. (a) full spectrum. (b) simulation with parameters (coupling constants $\times 10^{-4}$ cm^{-1}): g_{11}, 2.271; $g_{\perp}$, 2.063; A_{11} (^{63}Cu), 172.1; $A_{\perp}$(^{63}Cu), 15.9; A_{11}(^{14}N), 11.3; $A_{\perp}$(^{14}N), 14.7. (c) expansion of $g_{\perp}$ region. (d) simulation of (c) with parameters given in (b) above.

coupling. Such structure is not resolved on this resonance although its effects will contribute to the observed line shape.

In contrast, structure is clearly resolved in the perpendicular region and can be attributed to a mixture of ^{63}Cu ($I = {}^3/_2$) and ^{14}N ($I = 1$) hyperfine coupling. An excellent simulation (Figure 7; least-squares fitting parameter $L = 0.35 \times 10^{-3}$) required hyperfine coupling to a single ^{63}Cu and four ^{14}N atoms. The derived g values and coupling constants are given in Figure 7, while the line-width parameters are listed in the Experimental Section. The stick diagrams in Figure 7c,d show that the structure can be resolved into contributions from the highest field parallel resonance ($M_I = -{}^3/_2$) and from the four perpendicular resonances each split into nine components (relative intensities, 1:4:10:16:19:16:10:4:1), by interaction with four equivalent ^{14}N nuclei.

Simulations assuming coupling to three N atoms were significantly less satisfactory and those assuming two or one N were unsatisfactory.

The magnitude of $A_{11}(^{63}Cu)$ is typical of simple Cu^{II} complexes and very different from the characteristically small values [(30–100) $\times 10^{-4}$ cm^{-1}] characteristic of type I copper sites. The Blumberg–Peisach plots[55] correlate g_{11} and A_{11} (^{63}Cu) values with the nature of the four "in-plane" donor atoms. Cu^{II}-ADH falls in the regions defined for N_2O_2, N_3O, and N_4 donor sets and, interestingly, very close to the position of $[Cu(imidazole)_4(H_2O)_2]^{2+}$.[55,56]

Summary of M^{II}-ADH (M = Mn, Fe, Co, Ni, Cu) Data. The magnetic susceptibility, ESR, and Mössbauer data all point to the presence of high-spin six-coordinate sites influenced by a ligand field close to octahedral. The electronic spectra of M^{II}-ADH (M = Co, Ni) are closely related to those exhibited by the MN_4O_2 sites in crystalline $M(His)_2{\cdot}H_2O$. At least three and most probably four nitrogen ligands are observed directly via hyperfine structure in the ESR spectrum of Cu^{II}-ADH. Taken as a whole, the results strongly support the presence of a high-spin, six-coordinate ferrous site in the native enzyme. The three or four nitrogen ligands present would appear to be histidine residues, while the other ligands are most likely to be oxygens supplied by H_2O, aspartate, glutamate, or tyrosinate.

Influence of Substrates. Addition of coenzyme NAD^+ causes a dramatic change to the electronic spectrum of catalytically active Co^{II}-ADH (Table III; Figure 2 of ref 3). A limiting spectrum is obtained at Co:NAD^+ = 1:3.4 in which the absorption maximum shifts from 19 600 to 17 500 cm^{-1} and the molar absorptivity increases from 31.5 to 71 M^{-1} cm^{-1}. A coordination number cannot be assigned confidently, but the absence of significant absorption below 15 000 cm^{-1} does not support the presence of a five-coordinate site.[42] In HLADH, NAD^+ binds close to, but not directly to, the zinc atom inducing a conformational change in the protein chain close to the metal site.[57] A similar situation would explain the perturbation experienced by the Co^{II} site in the present case. This perturbation is also detected in the ESR (Table II; Figure 3b) and MCD[42] spectra at Co:NAD^+ = 1:3.4. In particular, computer simulation of the ESR spectrum (Table II; Figure 3) indicates an axially symmetric ligand field at the Co site.

The Mössbauer spectrum of the native enzyme exhibits subtle but apparently significant changes at Fe:NAD^+ = 1:3.4 (Table I). The half-widths of the components of the quadrupole doublet and the peak asymmetry, as well as the δ and ΔE_Q values, show small differences in comparison to Fe^{II}-ADH.

While the effect of NAD^+ is discernable in the spectroscopic properties of the active enzymes Fe^{II} and Co^{II}-ADH, it does not appear to affect those of the inactive enzymes. For example, NAD^+ does not perturb the electronic spectrum of Ni^{II}-ADH (Figure 6). The electronic spectra of M^{II}-ADH (M = Co, Ni) are similar to those of $M(His)_2{\cdot}H_2O$, but Co^{II}-ADH is active while Ni^{II}-ADH is not. The inactivity would seem to be related to the nature of binding of NAD^+ to Ni^{II}-ADH.

The inhibitory substrate *i*-PrOH has no effect on the electronic, ESR, or MCD spectrum of Co^{II}-ADH in the absence of NAD^+. In its presence, *i*-PrOH causes significant changes (Tables II and III; Figure 3c; Figure 2 of ref 3) with a limiting electronic spectrum being reached at Co:NAD^+:*i*-PrOH = 1:3.4:2600. In HLADH, alcohol or aldehyde substrates bind directly to the catalytic zinc atom.[57] However, the present system is complicated by the fact that *i*-PrOH at the above mole ratios in the presence of NAD^+ causes dissociation of tetrameric Fe^{II}- and Co^{II}-ADH, apparently into dimers.[2] Again, the effect is not seen in the absence of NAD^+. However, detailed interpretation must await further work.

Aerobic Inactivation of Fe^{II}-ADH. The native enzyme is not very stable as isolated, with a half-life of 5–10 h for active enzyme reconstituted from apoenzyme. The course of the inactivation was followed via Mössbauer spectroscopy.

Samples of apoenzyme (6.0×10^{-4} M) were reactivated with $^{57}Fe^{II}$ as $(NH_4)_2Fe(SO_4)_2$ solution and allowed to stand in air at 4 °C for 5, 20, and 76 h, respectively, with occasional stirring. The samples were then frozen and examined by Mössbauer spectroscopy at 77 K. After 5 h, a weak absorption was seen superimposed on the characteristic Fe^{II}-ADH spectrum and this feature had increased in relative intensity after 20 h. The enzyme activity had dropped to ~30%. Deconvolution provided the following parameters for the second species: δ, –0.12 (5) mm s^{-1}; ΔE_Q, 0.9 (1) mm s^{-1}.

After 76 h, the enzyme activity was zero and a new spectrum was present with parameters δ, 0.48 (1) mm s^{-1}, and ΔE_Q, 0.74 (2) mm s^{-1}, characteristic of a high-spin Fe^{III} center. The latter spectrum can be reproduced at 77 K after reconstituting apo-

(55) Peisach, J.; Blumberg, W. E. *Arch. Biochem. Biophys.* **1974**, *165*, 691–708.
(56) Bonomo, R. P.; Riggi, R.; Bilio, A. J. *Inorg. Chem.* **1988**, *27*, 2510–2512.
(57) Ohlendorf, D. H.; Lipscomb, J. D.; Weber, P. C. *Nature* **1988**, *336*, 403–405.

enzyme with $^{57}Fe(NO_3)_3$. At 4.2 K, the spectrum consists of a hyperfine-split sextet superimposed upon the 77 K doublet. The spectrum can be fitted precisely to a doublet (δ, 0.45 mm s^{-1}; ΔE_Q, 0.75 mm s^{-1}; 31% relative intensity) plus a hyperfine sextet (hyperfine field 44.1 T; δ, 0.52 mm s^{-1}; negative EFG; 69% relative intensity). Coexistence of such a hyperfine pattern and parent doublet is typical of high-spin Fe^{III} and is probably related to the relaxation rate rather than to the presence of two separate species. Indeed, a similar spectrum has been reported for Fe^{III}-substituted HLADH.[24]

The size of the hyperfine splitting is similar to that observed in the 4.2 K spectrum of Fe^{III}-protocatechuate 3,4-dioxygenase, which is now known[57] to feature an FeN_2O_3 site. While the exact nature of the Fe^{III}-containing ADH samples described above remains to be revealed, it nevertheless appears that an important consequence of aerobic inactivation of Fe^{II}-ADH is the oxidation of ferrous iron to ferric by dioxygen.

Comparison with Other Enzyme Systems. The high-spin FeN_3O_3 or FeN_4O_2 center suggested for Fe^{II}-ADH contrasts with the $Zn^{II}S_2NO$ site in the well-characterized enzyme HLADH.[58,59] The different nature of the sites is emphasized by comparison of the spectral properties of the Fe^{II}, Co^{II}, Ni^{II}, and Cu^{II} forms of each enzyme. The sites are so different that one is tempted to seek an alternative role for Fe^{II}-ADH, especially as non-heme iron enzymes are prominent in the metabolism of dioxygen. However, different organisms can evolve contrasting systems to carry out similar tasks. Examples of interest to the present work include hemerythrin (non-heme iron), hemoglobin (heme iron), and hemocyanin (copper) as dioxygen carriers and non-heme iron, manganese, and copper–zinc forms of superoxide dismutase.

The Mössbauer and magnetic parameters suggest that the active site in Fe^{II}-ADH is related to the ferrous sites detected in catechol 2,3-dioxygenase, proteocatechurate 3,4-dioxygenase, and SBL. The latter features a rhombically distorted six-coordinate site with three to five histidine ligands and at least one H_2O ligand.[36,60-62] Both Fe^{II}-ADH and SBL autoxidize fairly slowly, perhaps a consequence of the high coordination number.

The similarity of the electronic spectra of Co^{II}-ADH and Co^{II}-glyoxylase I (Table III) suggest that the two sites are closely related. At least one nitrogen ligand and two water ligands have been detected in the Cu^{II} and Mn^{II} forms of glyoxylase I.[40,63]

Acknowledgment. P.T. is grateful for the award of a Commonwealth Postgraduate Scholarship. K.S.M., E.N.B., and G.R.H. acknowledge financial support from the Austrialian Research Council, the National Research Fellowship Scheme, and Monash University Special Research Grants. We thank J. D. Cashion and J. R. Pilbrow, Monash University, for access to the Mössbauer and ESR facilities.

Appendix

Magnetic susceptibility data were analyzed by software developed for the VAX/VMS system. The two major parts are MATRIX, which calculates matrix elements for any Hamiltonian, and MAGB, which calculates, predicts, and fits energies, wave functions, magnetic susceptibilities, etc. for that Hamiltonian. Copies may be obtained from E.N.B. or K.S.M.

The data for Fe^{II}-ADH was fitted to Hamiltonian 3 operating on a set of $^5T_{2g}$ basis functions:

$$H = -\lambda\bar{L}\bar{S} + \frac{\Delta}{9}(3\bar{L}_z^2 - \bar{L}(\bar{L}+1)) + \frac{R}{12}(\bar{L}_+^2 + \bar{L}_-^2) + \beta(\kappa\bar{L} + 2\bar{S})\bar{H} \quad (3)$$

Use of a least-squares fitting routine showed that the calculated values of susceptibility were sensitive to variations in Δ, R, and λ. The best-fit κ value was always close to 1.

The quality of fit in the least-squares fitting routine was estimated by the discrepancy index, $I = 100[\sum(\chi_{obs} - \chi_{calc})^2/\sum\chi_{obs}^2]^{1/2}$.

The data for Co^{II}-ADH was fitted to Hamiltonian 3 operating on a set of $^4T_{1g}$ basis functions.[31] For best fit ($I \sim 7\%$): (i) κ is again close to 1; (ii) the axial parameter Δ is small in magnitude, 70 ± 30 cm^{-1}, with positive or negative values giving equally good fits; (iii) the rhombic parameter R does not influence the fit sensitivity with values of 0–40 cm^{-1} being acceptable; (iv) the best fit value of λ is about -50 cm^{-1}, which is low and much smaller than anticipated for six-coordinate Co^{II} complexes.[31]

It is unlikely that the low value of λ is real. Its apparent magnitude, like the uncertainty in the sign of Δ, is probably a reflection of the experimental error in μ_{Co} at the high-temperature end of the accessible range 4.2–52.3 K (Figure 2), as well as the fact that parameter variation is less sensitive in this range for a $^4T_{1g}$ state than it is in the higher 50–300 K range. Furthermore, the present calculation uses only a limited basis set[31] and no allowance is made for zero field splitting of the ground sublevel.

The data for Mn^{II}-ADH and Ni^{II}-ADH were fitted to spin Hamiltonian 4:

$$H = D[\bar{S}_z^2 - \tfrac{1}{3}\bar{S}(\bar{S}+1)] + g\beta\bar{H}\bar{S} \quad (4)$$

The best-fit parameters are given in the text.

(58) Zeppezauer, M. In *The Coordination Chemistry of Metalloenzymes*; Bertini, I., Drago, R. S., Luchinat, C., Eds.; Reidel: Dordrecht, The Netherlands, 1983; pp 99–122.
(59) Bränden, C.-I.; Jörnwall, H.; Eklund, H.; Furugren, B. In *The Enzymes (3rd Ed.)* Boyer, P. D., Ed.; Academic Press: New York, 1975; Vol. 11, pp 103–190.
(60) Feiters, M. C.; Al-Hakim, M.; Navaratnam, S.; Allen, J. C.; Veldink, G. A.; Vliegenthart, J. F. G. *Recl. Trav. Chim. Pays-Bas* **1987**, *106*, 227.
(61) Nelson, M. J. *J. Am. Chem. Soc.* **1988**, *110*, 2985–2986.
(62) Navaratnam, S.; Feiters, M. C.; Al-Hakim, M.; Allen, J. C.; Veldink, G. A.; Vliegenthart, J. F. G. *Biochim. Biophys. Acta* **1988**, *956*, 70–76.
(63) Sellin, S.; Erikkson, L. E. G.; Mannervik, B. *Biochemistry* **1987**, *26*, 6779–6784.